

# Patagonia's Chubut River: Overview of the Main Hydrological and Geochemical Features



Pedro. J. Depetris and Andrea I. Pasquini

**Abstract** The Chubut River's mean annual discharge is  $\sim 1.1 \text{ km}^3$  ( $\sim 35 \text{ m}^3 \text{ s}^{-1}$ ), contributes  $\sim 2\%$  to Patagonia's total freshwater discharge, and ranks far behind the mighty Negro River ( $\sim 32 \text{ km}^3 \text{ y}^{-1}$ ). In a semiarid scenario, the river has a mountainous active basin, low runoff ( $< 3.5 \text{ mm y}^{-1}$ ), and a scanty specific water yield ( $1.1 \text{ L s}^{-1} \text{ km}^{-2}$ ). The seasonal Kendall trend test shows that discharges during the low-water months (Jan.–Mar., May) have been significantly decreasing during the last decades.  $\text{Ca}^{2+}$ – $\text{HCO}_3^-$  are the governing ions in the headwaters but the composition gradually shifts to a  $\text{Na}^+$ -type toward the lowermost reaches. Numerous Andean glaciers suggest that subglacial oxidation of pyrite may be an active solute-supplying mechanism. Silicate hydrolysis and limestone dissolution—implied by non-radiogenic  $^{87}\text{Sr}/^{86}\text{Sr}$  ratios—are the processes ruling chemical weathering. The Chubut is a mesotrophic river, with a moderate organic load (mean TOC  $\sim 290 \mu\text{mol L}^{-1}$ , and mean yield  $\sim 10.5 \text{ mmol m}^{-2} \text{ y}^{-1}$ ;  $\sim 60\%$  accounted for by DOC). Suspended sediment yield at Los Altares ( $\sim 14 \text{ T km}^2 \text{ y}^{-1}$ ) and in the lowermost reach ( $\sim 25 \text{ T km}^2 \text{ y}^{-1}$ ) indicate a relatively low denudation. The alteration index of riverbed sediments (mean CIA  $\approx 55$ ) suggests scarce weathering; REE spider diagrams of sediments shows a signature compatible with continental island arcs.

**Keywords** Water chemistry · Geochemistry · Hydrology · Denudation · Solute provenance · River sediments

---

Pedro. J. Depetris  
Academia Nacional de Ciencias, Córdoba, Argentina

A. I. Pasquini (✉)  
Escuela de Geología, Facultad de Ciencias Exactas, Físicas y Naturales, Universidad Nacional de Córdoba, Córdoba, Argentina  
e-mail: [apasquini@unc.edu.ar](mailto:apasquini@unc.edu.ar)

Centro de Investigaciones en Ciencias de La Tierra, Consejo Nacional de Investigaciones Científicas y Técnicas, and Universidad Nacional de Córdoba, Córdoba, Argentina

## 1 Introduction

Due to the windy and arid characteristics ruling climate in southern South America's Atlantic seaboard plateau, Patagonia is considered among the unusual regions of the Earth. Several reasons make Patagonia an especially interesting expanse whose study could improve, for example, our understanding of climate change, particularly in connection with hydrological and geochemical issues. Its vast territory of over one million square kilometers consists of the southernmost stretch of the Andes, in the western part (with chains of about 2000–3000 m above the sea level (a.s.l.), and peaks that reach ~3700 m), and deserts, steppes and grasslands in the eastern plateau (~200–~600 m a.s.l.). The Colorado River (36°52' S, 69°45' W), with Andean **headwaters**, is usually considered Patagonia's northern boundary in the Argentine territory.

With ~1.1 km<sup>3</sup>, the Chubut ranks, in terms of annual discharge, as the fourth largest Patagonian river, behind the Negro, Santa Cruz, and Colorado. Joined together, the drainage nets of the Chubut and Senguerr-Chico rivers occupy about 60% of the surface area of the Argentine province named after it, which was originally organized as the National Territory of Chubut in 1884, and colonized the following year by Welsh immigrants.

Several authors have studied varied aspects in connection with the hydrological features of the Chubut River (e.g. Moyano and Moyano 2013; Pasquini and Depetris 2007; Depetris and Pasquini 2008), and its geochemical/biogeochemical characteristics (e.g. Sastre et al. 1998; Pasquini 2000; Gaiero et al. 2002, 2003; Pasquini et al. 2005; Depetris et al. 2005).

Due to the dynamics of natural and/or anthropogenic factors, rivers tend to show modifications in their main characteristics (i.e. discharge regime, physicochemical and/or biological features, etc.). We are, hence, herein updating hydrological and geochemical information on Patagonia's Chubut River.

### 1.1 Physiographic and Climatic Features

The Chubut<sup>1</sup> River drainage basin is an east-flowing arid Patagonian fluvial system (Fig. 1). Its drainage area is ~53,200 km<sup>2</sup> (Subsecretaría de Recursos Hídricos 2002), and its main stem, the Chubut River, has an approximate length of ~800 km and headwaters in the Cerro de las Carreras (41° S, 71°19' W)—at ~1800 m a.s.l.—, in Argentina's Río Negro Province. The main tributaries in the upper drainage are the Ñorquinco and Chico del Norte rivers, inflowing from the north, and the Tecka-Gualjaina River, joining the system from the south (Fig. 1). The Florentino Ameghino dam forms a reservoir lake (43°41' S, 66°29' W). The Chico del Sur River (i.e. a prolongation of the Senguerr River) used to join the Chubut River **upstream** from the

---

<sup>1</sup> Chubut comes from the aboriginal (i.e. tehuelche) word *chupat*, which means “transparent”. Welsh settlers called the river “*Afon camwy*”, meaning “twisting river”.

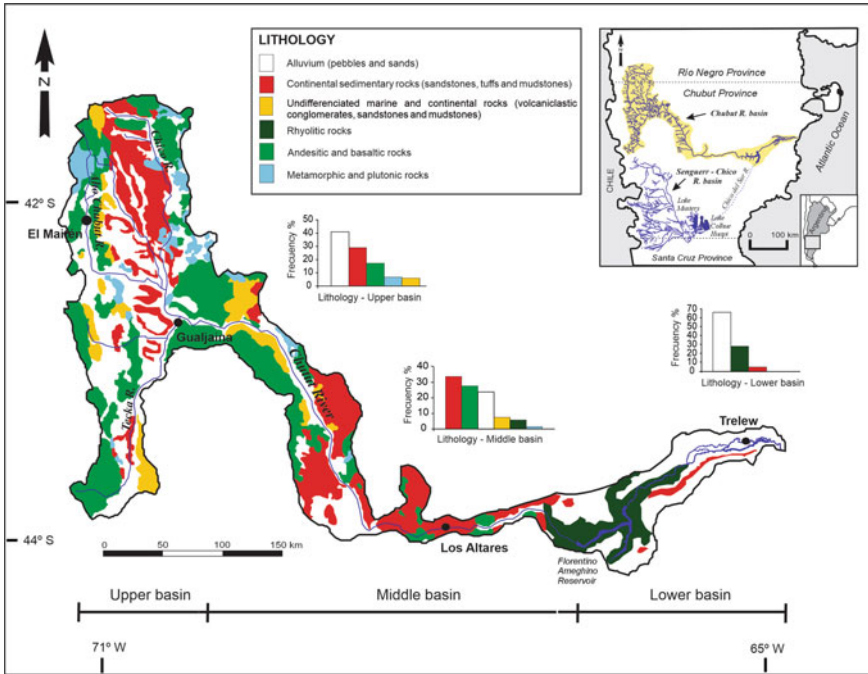


**Fig. 1** Schematic map of Patagonia’s Chubut River drainage basin showing an outline of the most abundant rock types. Histograms show the relative abundance (percent) of major rock types in the upper, middle, and lower river reaches

present location of the dam. Currently, this river, fed by the lakes Munster and Colhue Huapi, has been dammed by accumulated eolian debris which, almost permanently, obstruct its normal flow. The Chubut River reaches the Atlantic forming a small estuary at Bahía Engaño, near Rawson, the provincial capital.

The western headwaters of the Chubut River drainage basin are typified by mountainous north–south ranges (~500 and ~1800 m a.s.l.). The mean slope for the upper catchments is about 20%. The central drainage basin carves the Patagonian tableland (~200 and ~600 m a.s.l.), without receiving any significant tributary. An alluvial plain and fluvial terrace are the outstanding features in the lower drainage basin (~20 and ~150 m a.s.l.).

The Andes in Chubut’s territory are separated by wide, deep, east–west transverse valleys. These valleys are occupied by glacial lakes and rivers that cross the Andes and flow east, to the Pacific Ocean.

The most distinctive climatic characteristics in the Chubut River drainage basin are scarce atmospheric precipitations and their marked negative gradient in short distances. In the headwaters, for example, mean annual rain- and snowfall is 500–600 mm, whereas 200 km to the east, near the confluence with the Gualjaina River

(Fig. 1), it barely reaches 100 mm. In the central basin, the mean annual rainfall is ~150 mm and in the coastal zone it increases up to ~250 mm.

Atmospheric precipitations have a marked seasonal character, with most of the water volume recorded in winter (73% occurring between April and September). In contrast, along the coastal zone, most atmospheric precipitations occur in (austral) autumn and spring. Mean evapotranspiration exhibits an increasing trend from the Andean region (500–600 mm  $y^{-1}$ ) to the Atlantic coastal zone (700–800 mm  $y^{-1}$ ).

Mean annual temperatures vary between 8 and 9 °C in the west and center, and between 12 and 13 °C in areas close to the coast. The prevailing vegetation is a bushy or herbaceous steppe, with a vegetation cover that varies between 20 and 50%. Due to aridity, soils are scarcely developed in most of the drainage basin, with dominant sandy fractions in the profile. Aridisols are by far the overriding soil-types in the drainage basin (e.g. Bouza et al. 2017).

## 1.2 Geological Setting

The Chubut River drainage basin is located at the southern boundary of the North Patagonian or Somún Curá Massif. It is a plateau, surrounded by sedimentary basins, which rise 500–700 m above the surrounding topography, and reaches a maximum of 1200 m a.s.l. With an area of approximately 100,000 km<sup>2</sup>, it occupies most of the Argentine provinces of Río Negro and Chubut. An updated description of the continental crust of the northeastern region and, in general, Patagonia's main geological features, has been recently reported by Rapela and Pankhurst (2020) and in the references cited therein.

An abridged report of the geological setting of the Chubut River drainage basin has been described by Pasquini et al. (2005). Figure 1 shows a simplified geological scheme of the complex lithology of the Chubut River drainage basin which, for convenience, has been grouped into six major clusters. The dominant lithology in the upper basin are pebbles and sands, along with continental sedimentary rocks (sandstones, tuffs, and mudstones), which become dominant in the middle stretch (Fig. 1).

## 1.3 Methodology

The hydrological information was obtained from the data base operated by Argentina's *Secretaría de Infraestructura y Política Hídrica* (<http://bdhi.hidricosargentina.gob.ar>), and processed with standard statistical software.

The non-parametric **seasonal Kendall test** was employed to test for monotone trends in mean annual discharge time series. This test is a robust technique to detect and estimate linear trends and, also, was employed to seek significant trends in seasonal data with serial dependence (e.g. Hirsch and Slack 1984).

The chemical methodology employed to analyze water samples during the European Commission-funded PARAT Project (Contract CI1\*-CT94-0030) was described in Pasquini et al. (2005). Other cited references must be consulted whenever methodological information is required for data from alternative sources.

## 2 Hydrological Aspects

The hydrological behavior of the Chubut River mainly depends on rainfall and snowfall in the upper catchments. Most of the discharge is supplied by the upper Chubut River (i.e. 60–65% during the low-discharge period). There are indications, however, that the Chubut—as it probably happens with other Patagonian rivers—may receive groundwater supplies at different points along its middle and lower course. There is, for example, substantial evidence of submarine groundwater discharge in the coastal zone of Chubut and Santa Cruz provinces (42°–48° S) (Torres et al. 2018).

In the mountainous headwaters, atmospheric precipitations increase sharply in May (maximum mean precipitation) and June, during the austral fall and winter, and begin a gradual decrease that reaches its minimum in November (austral spring). The uppermost Chubut River gaging station (Estación Nacimiento, 41°43' S, 71°08' W) is operational since June 1967. During a period of over 50 years (i.e. until November 2019), the maximum recorded discharge ( $Q_{\max}$ ) was  $29.17 \text{ m}^3 \text{ s}^{-1}$ , whereas the minimum ( $Q_{\min}$ ) was  $0.41 \text{ m}^3 \text{ s}^{-1}$ .

Discharge data usually exhibit a log-normal statistical distribution. Therefore, the mathematical expectation is better approached by using the geometric mean discharge ( $Q_g$ ) (e.g. Davis 1986; Marsal and Merriam 2014).  $Q_g$  and the corresponding standard deviation ( $S_g$ ) at the Estación Nacimiento for the analyzed period was  $4.8 \pm 0.91 \text{ m}^3 \text{ s}^{-1}$ . The highest discharges are usually recorded in July–August (i.e. austral winter), due to rainfall and in October–November, as a result of snowmelt.

Rainfall and snowfall at the El Maitén gaging station (42°06' S, 71°10' W) follows a pattern similar to the one recorded at Nacimiento, although maximum mean precipitation occurs in June, with the minimum also in November. The station is located at ~720 m a.s.l. and the available discharge time series for the period 1953–2019 includes over 6800 instantaneous discharge measurements, with  $Q_{\max} \approx 240 \text{ m}^3 \text{ s}^{-1}$  and  $Q_{\min} \approx 1.9 \text{ m}^3 \text{ s}^{-1}$ .  $Q_g$  and the corresponding  $S_g$  is  $16.2 \pm 2.23 \text{ m}^3 \text{ s}^{-1}$ . Therefore, 95% of the compiled data is comprised within  $Q_g \pm 2S_g$ :  $11.7 \text{ m}^3 \text{ s}^{-1} < Q_g < 20.7 \text{ m}^3 \text{ s}^{-1}$ .

The Los Altares gaging station is placed in a semi-arid region, on the southern margin of the Chubut River, about 230 km from Trelew (to the E), and 323 km from Esquel (to the W). The wild landscape is known for its high cliffs and striking geomorphology. The Los Altares station (43°53'18.17" S, 68°23'57.81" W) is active since January 1943, record-keeping instantaneous discharges and other hydro-meteorological variables. Chubut River's mean annual discharge time series have been plotted in Fig. 2. The linear trend in the figure ( $p < 0.05$ ) shows that in 75 years, the mean annual discharge has decreased  $\sim 6 \text{ m}^3 \text{ s}^{-1}$  ( $\sim 800 \text{ L}$  per decade). Figure 3

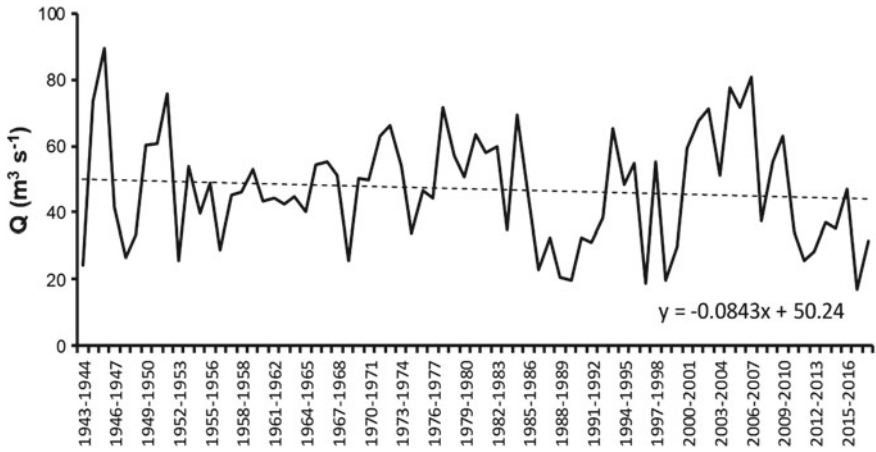


**Fig. 2** Mean annual discharge time series (1943–2018) of the Chubut River (middle reach) at Los Altares gaging station. The regression equation ( $p < 0.1$ ) suggests that the (arithmetic) mean annual discharge has decreased  $\sim 6 \text{ m}^3 \text{ s}^{-1}$  in 75 years

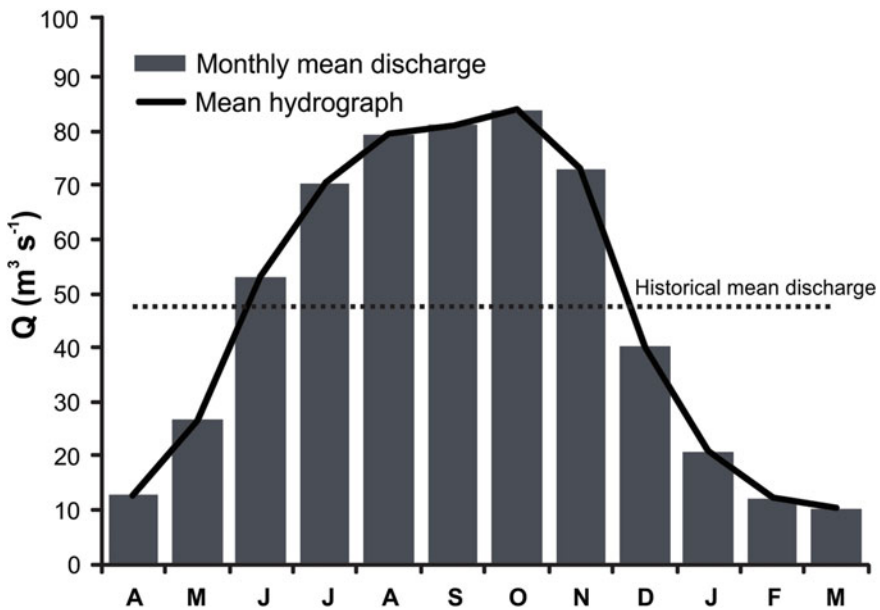


**Fig. 3** Middle Chubut River’s synthetic hydrograph at Los Altares ( $\sim 270 \text{ km}$  upstream the mouth;  $625 \text{ m a.s.l.}$ ). The graph shows the (arithmetic) mean historical discharge ( $\sim 47 \text{ m}^3 \text{ s}^{-1}$ ) for 1943–2018, and the (arithmetic) mean monthly discharges for the average hydrological year

shows the mean annual hydrograph for the series of monthly mean discharges (i.e. period of 1943–2018), with maximum discharges occurring during austral spring. The average discharge (i.e. arithmetic mean) for the period was  $47.04 \text{ m}^3 \text{ s}^{-1}$ , whereas the annualized discharge was  $14.84 \text{ km}^3$ , the specific water yield was  $2.87 \text{ L s}^{-1} \text{ km}^{-2}$ , and runoff exceeded  $9 \text{ mm y}^{-1}$ . In the studied time series, instantaneous  $Q_{\max}$  was  $524 \text{ m}^3 \text{ s}^{-1}$ , and  $Q_{\min}$   $2.1 \text{ m}^3 \text{ s}^{-1}$ .

As it happens with the upstream discharge time series, the statistical distribution is markedly log-normal. The Chi-square test performed to verify log-normality (317.14) exceeds the critical value for 9 of freedom and  $p < 0.001$ . Hence,  $Q_g \pm S_g$  at Los Altares is  $35.9 \pm 2.72 \text{ m}^3 \text{ s}^{-1}$ , which is lower than the arithmetic mean calculated above. The conversion to a Gaussian distribution of the discharge time series (1943–2018) allows to estimate that 95% of the data in the historical series falls within the range  $30.5 < Q_g < 41.4 \text{ m}^3 \text{ s}^{-1}$ .

The seasonal Kendall trend analysis (Kendall 1975; Hirsch and Slack 1984) is a non-parametric statistical tool that allows establishing monotonic trends in time series. The use of the technique at Los Altares shows a statistically significant discharge decrease ( $p < 0.05$ ) during January-March and May (i.e. the months with low-water flow) (Table 1).

The Chubut's lower stretch originates at the reservoir lake formed by the Florentino Ameghino dam (Fig. 1), which became operative in 1963, 130 km west of the city of Trelew (i.e. Gaiman Department). The reservoir lake has a surface area of  $\sim 70 \text{ km}^2$ , a mean maximum depth of  $\sim 25 \text{ m}$ , and a storage capacity of  $\sim 16 \text{ km}^3$  of water, which is mostly used for irrigation, and power generation.

The Valle Inferior ( $43^\circ 17' 35.13'' \text{ S}$ ,  $65^\circ 29' 54.72'' \text{ W}$ ) gaging station is located approximately 90 km **downstream** the Florentino Ameghino dam and less than

**Table 1** Seasonal Kendall test: Chubut River monthly mean discharges at Los Altares

Month	N	Kendall t	$p^*$
January	75	-2.132	<b>0.01651</b>
February	75	-2.461	<b>0.00693</b>
March	75	-2.159	<b>0.01541</b>
April	75	-0.567	0.28527
May	75	-1.935	<b>0.02649</b>
June	75	-0.814	0.20776
July	75	-0.654	0.25651
August	75	-0.174	0.43100
September	75	0.897	0.18497
October	75	-0.851	0.19743
November	75	-1.505	0.06617
December	75	-1.606	0.05418
<b>Total</b>	900	-1.819	<b>0.03445</b>

\* Statistically significant parameters in bold ( $p < 0.05$ )

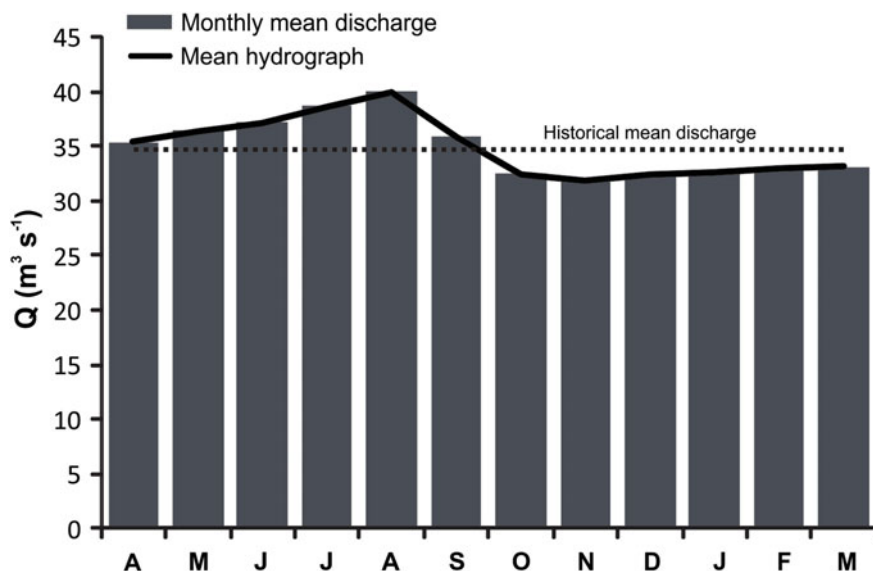


**Fig. 4** Lower Chubut River's synthetic hydrograph at Valle Inferior. The graph shows the (arithmetic) mean historical discharge ( $\sim 35 \text{ m}^3 \text{ s}^{-1}$ ) for the recorded period, and the (arithmetic) mean monthly discharges for the average hydrological year

50 km upstream from the Chubut's estuary in the Atlantic Ocean. It is in operation since 1993. The discharge time series (i.e. 1993–2018) is summarized in the synthetic hydrograph of Fig. 4, which shows the discharge modulation imposed by the dam. The annual mean discharge (i.e. arithmetic mean) at Valle Inferior is  $34.9 \pm 14 \text{ m}^3 \text{ s}^{-1}$ , and the mean annual flow is  $1.1 \text{ km}^3$ . The specific water yield is only  $1.1 \text{ L s}^{-1} \text{ km}^{-2}$ , whereas runoff is slightly less than  $3.5 \text{ mm y}^{-1}$ . These parameters, considerably lower than those determined in the middle stretch, are mainly the joint consequence of evapotranspiration, consumptive use of water, and the conveyance of river water to the aquifers (Hernández et al. 1983). The negative trend of mean discharges is clearly exhibited in Fig. 5. In 25 years, annual mean discharges have decreased at a mean rate of  $\sim 7.8 \text{ m}^3$  per decade. This scenario of water loss can also be ascertained in lower graph of Fig. 5, which shows the discharge difference between Los Altares and Valle Inferior ( $\Delta Q$ ) for the 1993–2018 record period.

### 3 Geochemical Perspective

Lithology, climate, biota, and relief are the key factors determining rock **weathering** on the Earth's surface (e.g. Depetris et al. 2014). The intensity of physical, biological and chemical weathering, on the other hand, determines the prevailing characteristics of dissolved and particulate byproducts that rivers transport to world oceans. In the



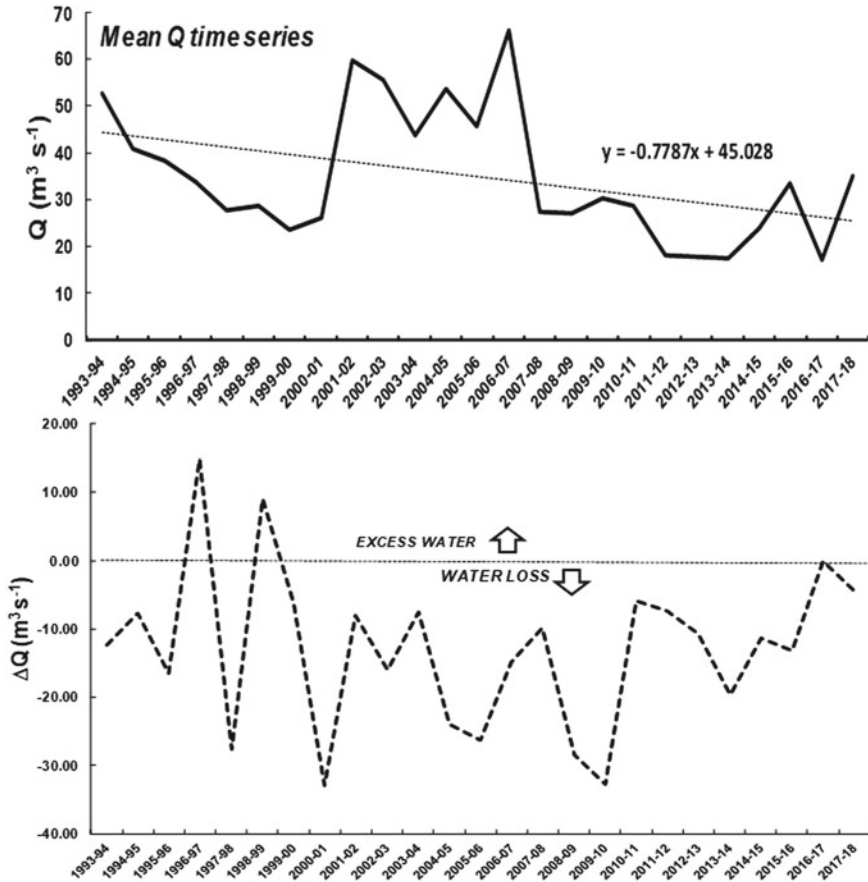


**Fig. 5** Mean annual discharge time series of the Chubut River (lower reach) at Valle Inferior gaging station, for the 1993–2018 period (upper graph). The regression equation implies that the (arithmetic) mean annual discharge has decreased  $\sim 20 \text{ m}^3$  in 25 years.  $Q$  between Los Altares and Valle Inferior gaging stations, for the same period time (lower graph), showing a significant discharge decrease for Chubut’s lower stretch during most of the time interval

Chubut River drainage basin, these three processes are significant in the mountainous headwaters, but it is clear that—considering extra-Andean Patagonia’s prevailing arid characteristics—physical (or mechanical) weathering becomes more important than the other two processes in its middle and lower reaches. All things considered, the Chubut River is subjected to a *weathering-limited regime* (i.e. denudation remains limited by the rate of rock weathering) in the sense of Carson and Kirkby (1972).

### 3.1 Main Characteristics

In terms of chemical equivalents, the Chubut River upper catchments (i.e. tributaries and the main channel) are generally characterized by  $\text{Ca}^{2+} > \text{Na}^+ > \text{Mg}^{2+} > \text{K}^+$ , and by  $\text{HCO}_3^- > \text{SO}_4^{2-} > \text{Cl}^-$ , among negatively charged species (Table 2). This chemical signature changes in the lower course, following the order of abundance  $\text{Na}^+ > \text{Ca}^{2+} > \text{Mg}^{2+} > \text{K}^+$ , and  $\text{HCO}_3^- > \text{Cl}^- \geq \text{SO}_4^{2-}$  (Table 3). The total dissolved solids (TDS) concentration in the Chubut River system usually fluctuates between 50 and 80 mg L<sup>-1</sup> in the upper reaches, and between 110 and 160 mg L<sup>-1</sup> at Los Altares. Typical TDS concentrations in the Gaiman–Rawson section (i.e. near the mouth) frequently oscillate in the 250–450 mg L<sup>-1</sup> range. In the headwaters (i.e. Tecka-Gualjaina and Lepá rivers), TDS concentrations are usually logged in the 60–150 mg L<sup>-1</sup> range. The TZ<sup>+</sup> parameter [TZ<sup>+</sup> (meq L<sup>-1</sup>) = (2Ca<sup>2+</sup>) + (2Mg<sup>2+</sup>) + (Na<sup>+</sup>) + (K<sup>+</sup>)] (e.g. Meybeck 2005) can be used with advantage to geochemically classify most Chubut River waters.

The Piper diagram (Fig. 6) shows a trend in the compositional triangle of major ions that begins in the Andean core—where lakes and rivers draining toward the Pacific Ocean are located—, revealing a dominant Ca<sup>2+</sup> > Mg<sup>2+</sup> composition. The trend drifts towards a slight relative increase of Mg<sup>2+</sup> in the upper Chubut and Senguerr rivers, which becomes increasingly dominated by (Na<sup>+</sup> + K<sup>+</sup>) in the Chubut's lower reaches. At the Musters and Colhué Huapi lakes begins the terminal phase of the Senguerr-Chico endorheic system which, in chemical terms, is characterized by a net dominance of (Na<sup>+</sup> + K<sup>+</sup>). In short, the chemical evolution originates as a Ca<sup>2+</sup>-type, crosses the field where no particular cation is dominant, and ends as a Na<sup>+</sup>-type (i.e. K<sup>+</sup> is significantly less abundant).

The anions show a similar trend that begins in the Andean domain with a HCO<sub>3</sub><sup>-</sup> control among the negatively charged species and shows, in the lower Chubut River and—more pronounced—in the Chico River, the increasing preeminence of Cl<sup>-</sup>. Among anions, the series begins in the HCO<sub>3</sub><sup>-</sup> type and ends in the no-dominant type realm (Fig. 6).

### 3.2 Provenance of Inorganic Dissolved Phases

Rock minerals have a variable susceptibility to weathering. The relative stability of the major rock-forming silicates during weathering is similar to Bowen's crystallization sequence (e.g. Langmuir 1997): the minerals that crystallize first in high-temperature magmas are those which are least stable when subjected to weathering. Thus mafic minerals (e.g. olivine, pyroxenes) usually weather more readily than felsic minerals (e.g. plagioclase, micas), and a Ca-rich plagioclase is generally weathered at a faster rate than a Na-rich plagioclase. Chemical weathering reactions fall into four

**Table 2** Major chemical characteristics of the upper Chubut River and tributaries\*

Date	E.C. ( $\mu\text{S cm}^{-1}$ )	pH	$\text{Cl}^-$	$\text{SO}_4^{2-}$	$\text{HCO}_3^-$	$\text{Ca}^{2+}$ ( $\mu\text{mol L}^{-1}$ )	$\text{Mg}^{2+}$	$\text{Na}^+$	$\text{K}^+$	$\text{SiO}_2$	$\text{TZ}^+$ ( $\mu\text{eq L}^{-1}$ )
Dec '96 <sup>a</sup>	166	8.6	83	158	1390	492	196	518	32	220	1926
Mar '97 <sup>b</sup>	58.7	7.45	13	24	566	200	65	108	13	190	651
Dec '96 <sup>c</sup>	193	8.53	149	92	1750	457	206	874	45	352	2245
Dec '96 <sup>d</sup>	33.4	7.72	20	16	288	99	34	86	9	340	361
Mar '97 <sup>e</sup>	178.2	7.97	195	147	1490	521	151	383	34	252	1761
Mar '97 <sup>f</sup>	252	7.72	245	246	2039	692	256	594	41	270	2531

\* Modified from Pasquini et al. (2005)

<sup>a</sup>Chubut (P. de Indios); <sup>b</sup>Chubut (El Maitén); <sup>c</sup>Mayo (R. Mayo); <sup>d</sup>Senguerr (RP 22); <sup>e</sup>Lepá (RN 40); <sup>f</sup>Gualjaina (Gualjaina)

**Table 3** Major chemical characteristics of Chubut River at Trelew (~23 km from mouth)\*

Date	E.C ( $\mu\text{S cm}^{-1}$ )	pH	Cl <sup>-</sup>	SO <sub>4</sub> <sup>2-</sup>	HCO <sub>3</sub> <sup>-</sup>	Ca <sup>2+</sup> ( $\mu\text{mol L}^{-1}$ )	Mg <sup>2+</sup>	Na <sup>+</sup>	K <sup>+</sup>	SiO <sub>2</sub>	TZ <sup>+</sup> ( $\mu\text{eq L}^{-1}$ )
Sep '95	284	8.11	544	229	1680	562	183	1190	27	180	2707
May '96	250	7.54	413	198	1700	542	178	1090	24	203	2554
Sep '96	247	6.75	504	219	1670	584	193	1170	30	195	2754
Dec '96	331	8.5	925	357	1830	694	251	1710	32	218	3632
Mar '97	190	7.67	82	223	1570	536	235	549	35	253	2126
Dec '97	285	7.2	724	277	1755	569	191	1600	29	226	3149
Apr '98	315	7.53	793	330	1990	649	220	1730	33	175	3501
Nov '98	459	7.94	1450	522	2300	815	295	2520	40	171	4780
Apr '98	405	8.43	1420	440	1990	664	196	2620	58	231	4398
GM <sup>a</sup>	298		600.5	294	1819.9	618	213	1436.4	33.2	204.1	3132.4
SD <sup>b</sup>	2.1		2.4	1.4	1.1	1.2	1.2	1.6	1.3	1.2	2.7

\* Modified from Pasquini et al. (2005)

<sup>a</sup>Geometric mean; <sup>b</sup>Standard deviation

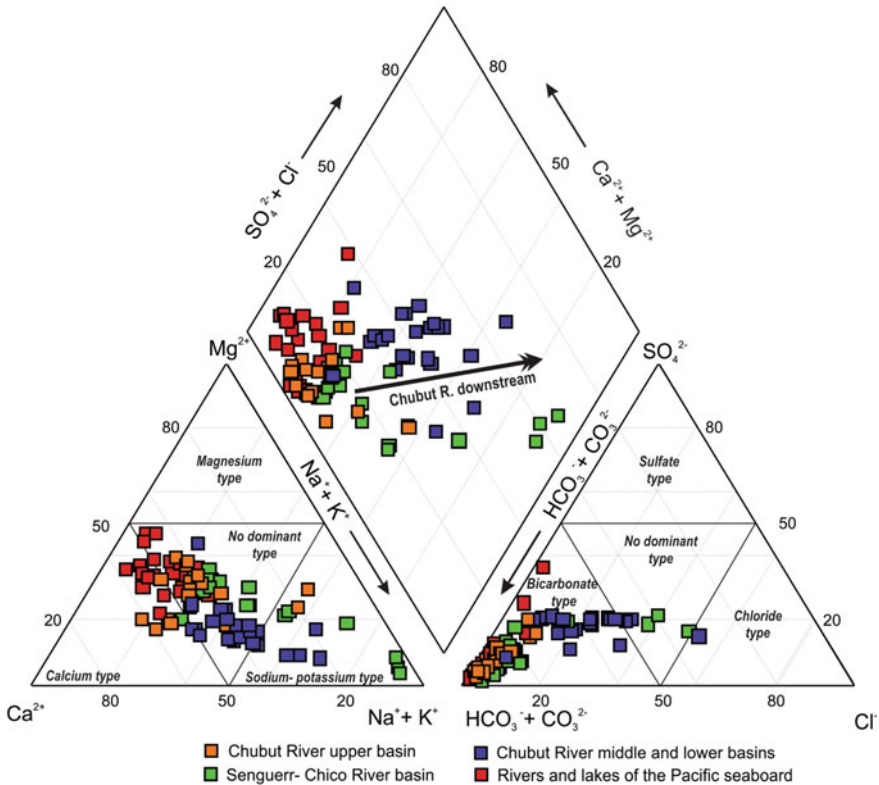


**Fig. 6** Diagram (Piper 1944) showing the chemical evolution of Chubut River waters from the upper to the middle and lower stretches. Senguerr-Chico drainage basin, as well as rivers and lakes draining to the Pacific seaboard are also included

major clusters: hydrolysis reactions; dissolution/precipitation reactions; redox reactions; hydration/dehydration and transformation processes. Different combinations among these processes are also possible.

Before entering the characteristics of weathering in the Chubut River drainage basin it must be kept in mind that the lithology of the upper catchments (i.e. where physical erosion is intense and atmospheric precipitations are higher) is dominated by alluvium, followed by continental sedimentary rocks (sandstones, tuffs, and mudstones), and volcanic rocks (i.e. andesitic and basaltic rocks) (Pasquini et al. 2005). With these broad guidelines in mind, it is possible to approach the sources of dissolved inorganic components in the Chubut River system.

The mixing diagram in Fig. 7 shows the relationship of  $Ca^{2+}$  and  $HCO_3^-$  (in  $\mu eq L^{-1}$ ), both normalized to  $Na^+$ , as measured in upper tributaries, and the upper and lower Chubut River (i.e. diagram after Gaillardet et al. 1999). Data of diluted lakes and rivers draining to the Pacific Ocean have been included for comparison (Scapini and Orfila 2001). The sampled rivers, lakes, and streams appear to have a

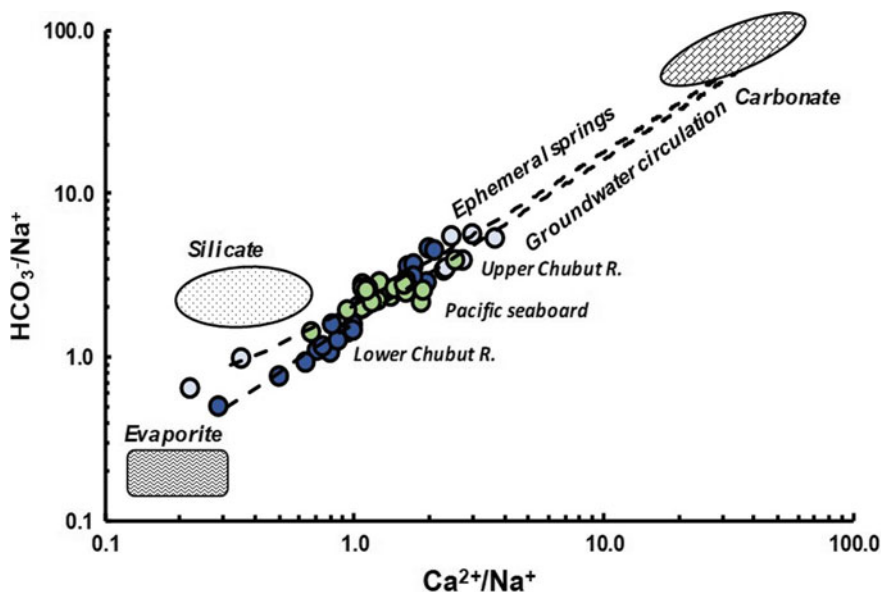
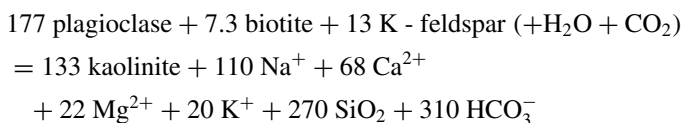
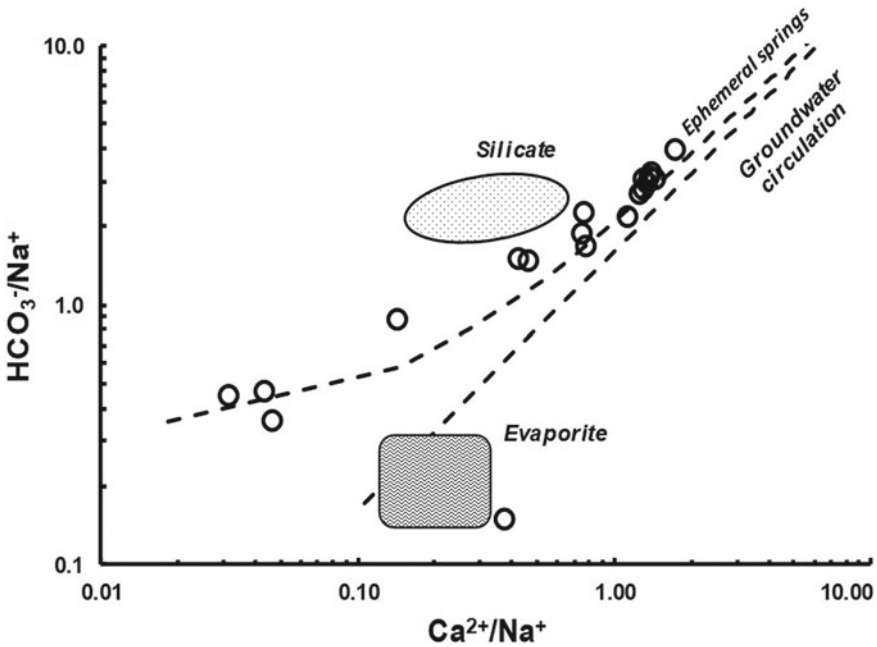


**Fig. 7** Variability of  $\text{Na}^+$ -normalized  $\text{Ca}^{2+}$  and  $\text{HCO}_3^-$  concentrations ( $\mu\text{eq L}^{-1}$ ) in the upper and lower Chubut River. Data from lakes and rivers draining to the Pacific Ocean included for comparison. Likewise, the evolution of weathering for Sierra Nevada (USA) rocks, as determined in ephemeral springs and deep groundwater (Garrels and Mackenzie 1967). Data uncorrected for rainfall; notice logarithmic axes. Diagram after Gaillardet et al. (1999)

more pronounced supply of weathering products from silicates and evaporites than of carbonates. It is also interesting to notice that some samples plot close to the line representing the composition of ephemeral springs, implying a relatively brief rock-water interaction, whereas other are closer to the composition of groundwater (i.e. longer rock-water contact time). The chemical data for springs and groundwater was collected in the Sierra Nevada (USA), and reflects the weathering of variable proportions of plagioclase, biotite, and K-feldspar (spring), and of plagioclase, biotite, and calcite (deep groundwater). The exercise (Garrels and Mackenzie 1967) was a reconstruction of source minerals, reproduced by Drever (1997). In ephemeral springs the overall reaction was:



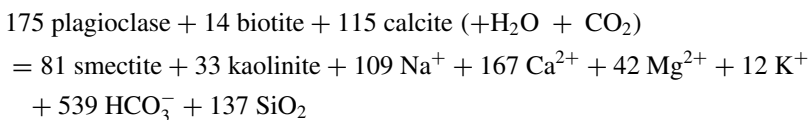
It appears, in terms of the  $\text{Na}^+$ -normalized  $\text{Ca}^{2+}$  and  $\text{HCO}_3^-$  concentrations, that the geochemical reconstruction computed by Garrels and Mackenzie (1967) fits reasonably well with both, springs with brief and groundwater with extended rock-water contact.



**Fig. 8** Variability of  $\text{Na}^+$ -normalized  $\text{Ca}^{2+}$  and  $\text{HCO}_3^-$  concentrations (in  $\mu\text{eq L}^{-1}$ ) in the Senguerr-Chico drainage basin. The geochemical signature of the flow-obstructed system contrasts markedly with the Chubut River. Other characteristics as in Fig. 7

In a similar albeit contrasting diagram, Fig. 8 shows the chemical composition of the Senguerr-Chico system. In this case, data falls close to the ephemeral spring composition of Garrels and Mackenzie (1967) (i.e. probably due to the deceptive effect of carbonate precipitation and the removal of  $\text{Ca}^{2+}$  and  $\text{HCO}_3^-$  from the solution). The system evolves towards a high ionic strength solution through the loss of water by evaporation that affects the Colhue-Huapi Lake and Chico River. A chemical divide, such as the one described by Drever (1997), surely functions and gypsum probably precipitates, leaving a solution which, in molar terms, is rich in  $\text{Na}^+$ ,  $\text{Cl}^-$ ,  $\text{SO}_4^{2-}$ ,  $\text{Ca}^{2+}$ ,  $\text{Mg}^{2+}$ , and  $\text{CO}_3^{2-}$  (Scapini and Orfila 2001).

The graph of  $\text{Ca}^{2+}/\text{Na}^+$  versus  $\text{Mg}^{2+}/\text{Na}^+$  (Fig. 9) shows a different scenario; where the weathering of Mg-bearing minerals seems to play a more important role in waters that probably undergo an extended rock-water contact. The reconstruction of weathering reactions during deeper circulation (Garrels and Mackenzie 1967), for example, show a more important character to Sierra Nevada's biotite and calcite as solute suppliers. In this case, the overall reaction was:



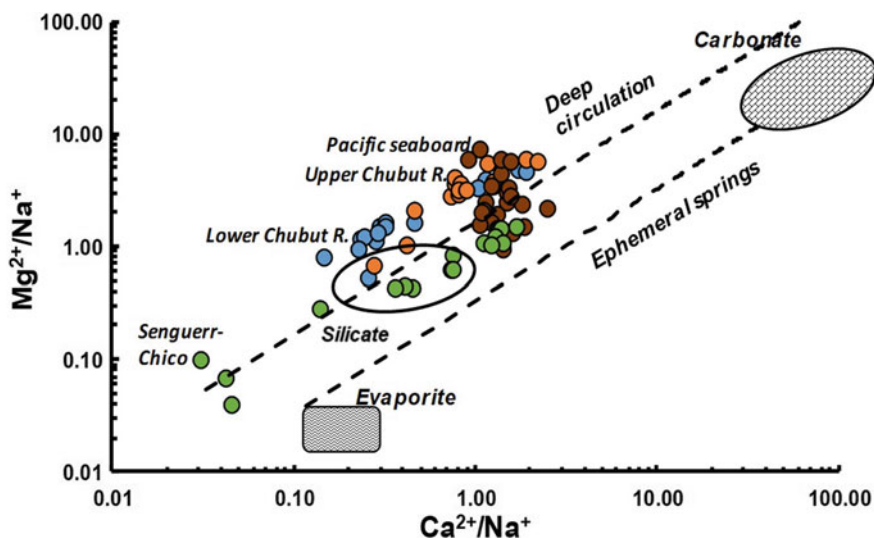
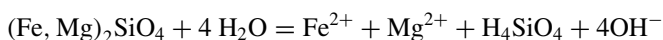


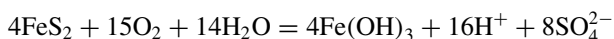
**Fig. 9** Variability of  $\text{Na}^+$ -normalized  $\text{Mg}^{2+}$  and  $\text{HCO}_3^-$  concentrations (in  $\mu\text{eq L}^{-1}$ ) in the upper and lower Chubut River. Data from the Senguerr-Chico system and the Pacific seaboard have been included for comparison. Other characteristics as in Fig. 7

Due to different geological conditions, there are minerals which are present in Chubut's drainage basin and absent or scarce in the Sierra Nevada and, hence, were not included in Garrels and Mackenzies' exercise. Such is the case, for example, of olivine, a mineral which hydrolyzes easily, common in mafic rocks, and a significant source of Mg and/or Fe:



In any event, it is important to look into the susceptibility of minerals to weathering, regardless of the rock involved.

In the Chubut River,  $\text{SO}_4^{2-}$  can be supplied by gypsum-bearing beds, by evaporites, or by redox reactions which involve sulfides, like pyrite. The latter is particularly important in glacial environments (e.g. Chillrud et al. 1994; Calmels et al. 2007). The reaction generates  $\text{H}_2\text{SO}_4$ , which assists in the dissolution of other minerals including carbonates, silicates and other sulfides:



This reaction is of particular importance in the subglacial and proglacial environments, where it is the dominant process producing solutes (Tranter 2005).<sup>2</sup> It must

<sup>2</sup> According to Argentina's glacier inventory (<https://www.argentina.gob.ar/ambiente/agua/glacias/res/inventario-nacional>), there are over 1500 ice and rock glaciers and snow buildups in Chubut's Andean region, covering a surface area of  $\sim 225 \text{ Km}^2$ .



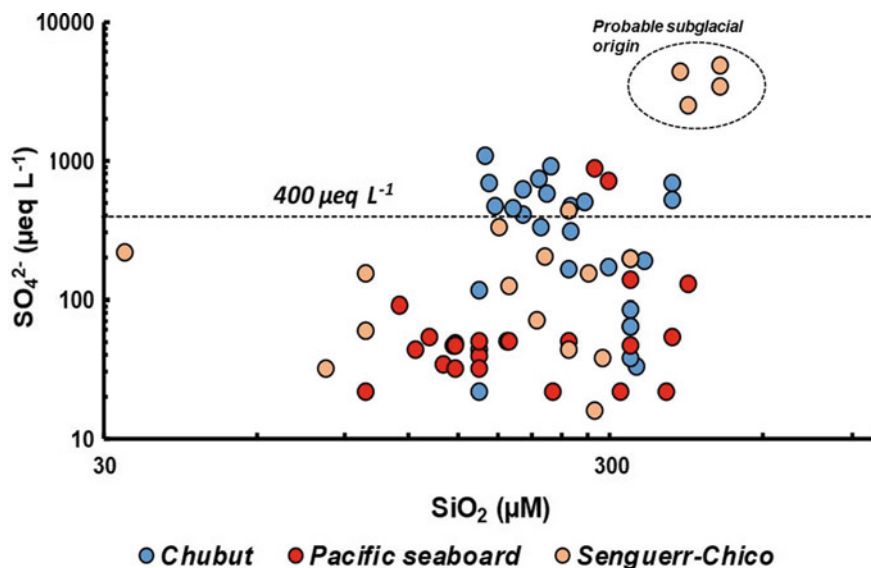
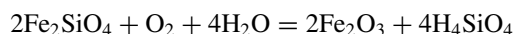


**Fig. 10**  $\text{SiO}_2$  versus  $\text{SO}_4^{2-}$  in the Chubut, Senguerr-Chico and in rivers and lakes of the Pacific seaboard. The graph shows the likely subglacial origin of Andean samples. Subglacial  $\text{SO}_4^{2-}$  may have contributed as well to the samples that plot above the  $400 \mu\text{eq L}^{-1}$  line

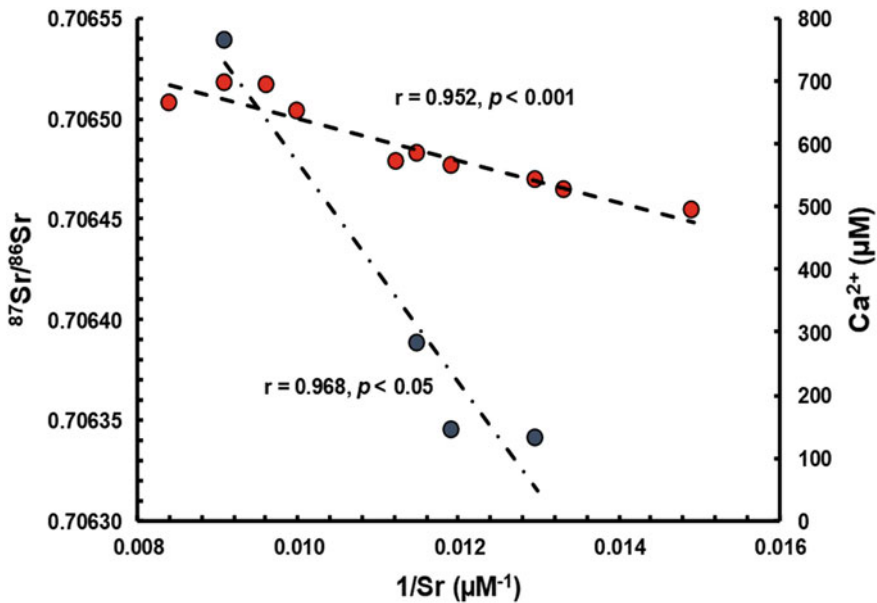
be kept in mind, however, that the maximum  $\text{SO}_4^{2-}$  concentration resulting from sulfide oxidation in  $\text{O}_2$ -saturated surface waters is  $\sim 400 \mu\text{eq L}^{-1}$ . Subglacial waters triplicate this concentration (Tranter 2005).

Figure 10 shows the variability of  $\text{SiO}_2$  and  $\text{SO}_4^{2-}$  concentrations in the Chubut River, in the neighboring Senguerr-Chico system, and in Andean lakes and rivers draining to the Pacific Ocean. High  $\text{SiO}_2$  and  $\text{SO}_4^{2-}$  concentrations in lakes pertaining to the Senguerr-Chico drainage suggest, for some samples, a likely subglacial origin (e.g. Tranter 2005). The  $\text{O}_2$ -supersaturated subglacial environment is propitious for the dissolution of other minerals besides pyrite. The alteration of the Fe-olivine (i.e. fayalite) is another example of dissolution in an  $\text{O}_2$ -rich environment, producing silica and Fe oxide:



Sulfate determined in other samples plotting above the  $400 \mu\text{eq L}^{-1}$  boundary may also be a mixture of subglacial  $\text{SO}_4^{2-}$ , outcropping salty groundwater, or from gypsum-rich beds and/or evaporites, whereas those falling below the boundary probably have a restricted  $\text{SO}_4^{2-}$  contribution from sulfide oxidation in surface waters saturated with  $\text{O}_2$ , along with other usual sources of  $\text{SO}_4^{2-}$ .

The Sr concentration and isotope composition of river waters are largely defined by the mixing of Sr derived from limestones and evaporites (i.e. low  $^{87}\text{Sr}/^{86}\text{Sr}$ , basically nonradiogenic), with Sr resulting from the weathering of silicate rocks (i.e.



**Fig. 11**  $^{87}\text{Sr}/^{86}\text{Sr}$  ratio (red symbols) and  $\text{Ca}^{2+}$  concentrations (dark symbols) plotted against  $1/\text{Sr}$ . The Sr isotopes suggest that  $\text{Ca}^{2+}$  is mostly supplied by limestone/carbonates

moderate to high  $^{87}\text{Sr}/^{86}\text{Sr}$ , radiogenic). In the Chubut River, the samples collected for isotopic analyses (Pasquini et al. 2005) showed low, nonradiogenic  $^{87}\text{Sr}/^{86}\text{Sr}$  ratios, which fluctuated between 0.706340 ( $\text{Rb}/\text{Sr} = 1.05 \times 10^{-3}$ ) and 0.706538 ( $\text{Rb}/\text{Sr} = 6.06 \times 10^{-3}$ ), thus suggesting an origin associated with limestones and evaporites. Sr frequently replaces Ca in crystalline structures and in the Chubut River;  $\text{Ca}^{2+}$  shows a significant covariation with Sr, thus denoting a common source (Fig. 11).

### 3.3 The Organic Load

Dissolved organic carbon/matter (DOC or DOM) is the result of organic matter decay. Autochthonous DOC (i.e. originating from within the river or lake) usually comes from aquatic plants or algae, whereas it is known as allochthonous DOC when it has a source external to the water body (i.e. organic soils and decaying terrestrial plants or organisms supplying carbon). In water bodies, DOC is complemented by readily decomposable particulate organic carbon (POC),<sup>3</sup> which is separated in water samples by sieving or filtration. This fraction includes organic detritus and plant

<sup>3</sup> Also reported as particulate organic matter or POM.

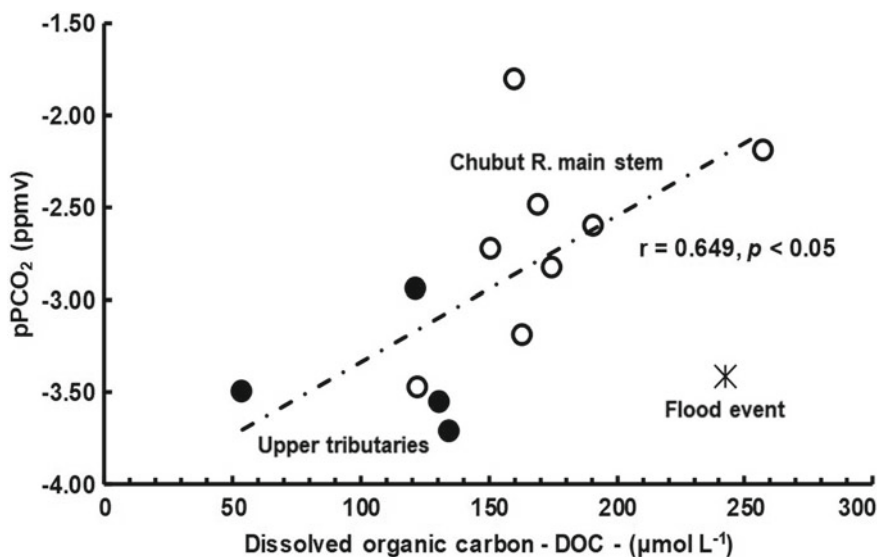


**Fig. 12** Plot of DOC versus pPCO<sub>2</sub> in the Chubut River (Black symbols are tributaries). The correlation suggests that ~40% of the variability in the CO<sub>2</sub> partial pressure may be accounted for by the respiration of DOC by heterotrophic bacteria. The outlier symbol corresponds to an exceptional flood event

material, algae, and pollen, partly decomposed through heterotrophic consumption (e.g. Killops and Killops 2005).

DOC, POC, and nutrients were determined in an earlier exploratory investigation on the biogeochemical typology of Patagonian rivers (Depetris et al. 2005). The study showed low DOC concentrations,<sup>4</sup> between 164 and 258 µmol L<sup>-1</sup> (i.e. mean concentration of 177 µmol L<sup>-1</sup>), thus reflecting the scarcity of organic-rich soils in Chubut's drainage basin. These concentrations allow to compute a DOC specific yield of only ~6.3 mmol m<sup>-2</sup> y<sup>-1</sup>.

As stated above, DOC in rivers usually consist of amounts of biodegradable residues which are rapidly recycled, and more important quantities of a biological refractory residue (e.g. poorly biodegradable leftovers of organisms). Labile organic matter, when respired by heterotrophic bacteria, produces CO<sub>2</sub>, in reactions like  $(\text{CH}_2\text{O})_n + n\text{O}_2 = n\text{CO}_2 + n\text{H}_2\text{O}$ .

There is, therefore, a frequent association in water bodies between DOC and the CO<sub>2</sub> partial pressure (i.e. PCO<sub>2</sub>). Figure 12 shows that in the Chubut River there is a significant positive correlation between DOC and pPCO<sub>2</sub> (i.e. pPCO<sub>2</sub> = log<sub>10</sub> PCO<sub>2</sub>), implying that a part of DOC (i.e. the labile fraction) is respired by

<sup>4</sup> The global DOC average concentration fluctuates between ~400 and 480 µmol L<sup>-1</sup> (Perdue and Ritchie 2005).

heterotrophs, increasing  $\text{PCO}_2$  in the water and thus affecting the concentration of dissolved inorganic carbon (DIC).<sup>5</sup>

Chubut's POC average concentration was  $\sim 110 \mu\text{mol L}^{-1}$  (i.e. fluctuating between 91 and  $141 \mu\text{mol L}^{-1}$ ), also drastically below mean global values (i.e. 330–400  $\mu\text{mol L}^{-1}$ , Perdue and Ritchie 2005). Therefore, POC's specific yield in the Chubut River was  $4.2 \text{ mmol m}^{-2} \text{ y}^{-1}$  (Depetris et al. 2005). Accordingly, mean total organic carbon (TOC) in the Chubut River was  $\sim 290 \mu\text{mol L}^{-1}$  (i.e.  $\sim 60\%$  accounted for by DOC), with a mean TOC yield of  $\sim 10.5 \text{ mmol m}^{-2} \text{ y}^{-1}$ .

In the Chubut River,  $\sim 2.5\%$  is the average relative contribution of POC to total suspended sediment (TSS), whereas the mean carbon to particulate nitrogen (PN) ratio in TSS (POC/PN) is  $\sim 5$ , thus suggesting a meager proportion of soil-derived carbon and a dominant autochthonous origin (i.e. mostly phytoplankton) for the organic matter transported downriver. With the exceptional instance of the Gallegos River,<sup>6</sup> this condition is common in the remaining Patagonian rivers (Depetris et al. 2005).

Summing up, the Chubut River is a mesotrophic water body (i.e. having a moderate amount of dissolved nutrients). Runoff was identified as the most important variable controlling the organic load (i.e. TOC) which is exported from Patagonia to the SW Atlantic Ocean's coastal zone (i.e.  $\sim 115 \cdot 10^9 \text{ g y}^{-1}$ ). The Chubut River is expected to supply  $\sim 3.5\%$  of such load (Depetris et al. 2005).

## 4 Sediments

Sediments in fluvial systems can be conveyed in suspension or as bed load along the riverbed. The term total suspended sediment (TSS) usually denotes solids coarser than  $0.45 \mu\text{m}$ . Bed load is difficult to measure and is usually assumed that it represents a relatively small fraction of the total sediment load (e.g.  $\sim 10\%$ , Milliman and Meade 1983), although it may be considerably higher in steep mountainous streams or somewhat lower in larger meandering rivers (Milliman and Farnsworth 2011). In any case, the flux of sediments to coastal oceans is taken as an image of the physical denudation of continents (Milliman and Farnsworth 2011, and references therein).

### 4.1 TSS Yield and Transport

The instantaneous discharge and TSS concentration in the Chubut River are non-linearly correlated, as measured at the Los Altares gaging station (<http://bdhi.hidricosargentina.gob.ar/>) (Fig. 13). The statistical analysis of the TSS data shows a significant log-normality and, hence, its geometric mean is  $\sim 196 \text{ mg L}^{-1}$  ( $N = 317$

<sup>5</sup>  $\text{DIC} = (\text{CO}_2^*) + (\text{HCO}_3^-) + (\text{CO}_3^{2-})$ , where  $(\text{CO}_2^*) = (\text{CO}_2) + (\text{H}_2\text{CO}_3)$ .

<sup>6</sup> Mean POC/PN  $\approx 10$ , thus suggesting a dominant origin in the terrestrial environment.

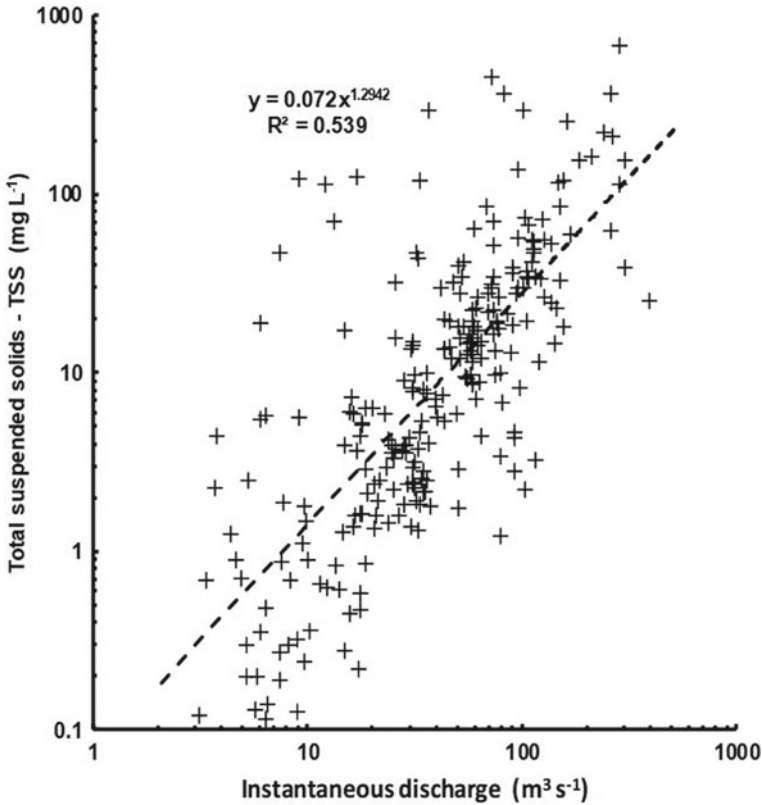


**Fig. 13** Chubut River at Los Altares. Nonlinear relationship between instantaneous discharge and TSS concentration. Notice that some storm events may determine TSS concentrations  $\sim 1 \text{ g L}^{-1}$ . Both axes are logarithmic

measurements). The lower quartile (i.e. 25% of the data is below) is  $\sim 71 \text{ mg L}^{-1}$ , whereas the upper quartile (i.e. 75% of the data lies below) is  $\sim 443 \text{ mg L}^{-1}$ . Clearly, the Chubut River is subjected to sporadic storm events that trigger very high TSS concentrations (e.g. over  $2 \text{ g L}^{-1}$ ).

On the basis of the above calculated  $Q_g$  at Los Altares (i.e.  $\sim 36 \text{ m}^3 \text{ s}^{-1}$ ) it is possible to compute a mean sediment transport rate of  $\sim 222.5 \cdot 10^3 \text{ T y}^{-1}$  or  $610 \text{ T d}^{-1}$ . It is possible, however, that during torrential storms the daily transport exceeds 7000 T. The resulting mean sediment yield at Los Altares is  $\sim 14 \text{ T km}^2 \text{ y}^{-1}$  (i.e. a measure of relatively low denudation). It is worth mentioning that a significant portion of the sediment load generated in the upper basin is retained at the Florentino Ameghino reservoir lake and—given the scarce vegetation cover, and the bare and loosened sediment outcrops that predominate in the lower valley—, more sediment is likely eroded,

added to the sediment load that bypasses the dam, and consequently transferred downstream, to the coastal zone.<sup>7</sup>

Pasquini et al. (2005) studied the nature of weathering, denudation, and the provenance of river bed sediments in the Chubut River system. A rating curve computed with data collected at the city of Trelew (i.e. ~25 km upstream the mouth) allowed to approach the mean TSS concentration. The equation  $[TSS (mg L^{-1}) = 0.8493Q^{1.3856}]$  delivered a concentration range that fluctuated between ~80 and ~190 mg L<sup>-1</sup> for the most frequent discharges at that particular gaging station.

The denudation rate computed at the time for the total Chubut drainage basin was ~25 T km<sup>2</sup> y<sup>-1</sup>; the use of empirical models developed by Ludwig and Probst (1998) supplied denudation rates that fluctuated between 19 and 32 T km<sup>2</sup> y<sup>-1</sup>. The Chubut River supplies an estimated ~3% of the TSS exported from Patagonia to the SW Atlantic coastal zone (Depetris et al. 2005).

## 4.2 The Geochemical Signature of Sediments

Another finding was that the materials removed from the drainage basin and exported to the coastal zone are barely modified by chemical weathering (i.e. the mean **chemical index of alteration**—or **CIA**—of riverbed material is ~55, relatively close to 47, the mean value calculated by McLennan (1993) for the Earth's Upper Continental Crust—UCC-) and exhibit a typical chemical and mineralogical signature characteristic of volcanic arcs. Hence, in spite of flowing toward a passive margin, the sediment bed load retains a geochemical signature typical of active margins, as Potter (1994) pointed out. Moreover, Pasquini (2000), and Pasquini et al. (2005) highlighted the features indicative of repeated weathering, supporting the view that, in the Chubut River drainage basin, most materials may have passed at least twice through the exogenous cycle (i.e. sedimentary recycling). Gaiero et al. (2004) probed into the significance of the **rare earth elements (REE)** signature in Patagonian wind- and river-borne sediments as provenance tracers.

Figure 14 shows the upper continental crust (UCC)-normalized REE extended diagrams (i.e. *spidergrams*) of Chubut River bed and suspended sediments (TSS) (Pasquini et al. 2005). Bed sediments are more depleted in light REE (i.e. LREE, La–Gd) than the TSS and have a conspicuous Eu anomaly, similar to the one exhibited by a typical Andean andesite (i.e. Average Andean Arc—AAA-). The REE of TSS exhibit a flatter pattern, a slightly depleted in LREE and enriched in heavy REE (i.e. HREE, Tb–Lu), and most plot above the Sample/UCC line. In general, they resemble the post-Archean Australian shale (PAAS), with a barely discernible Eu anomaly. Figure 14 ultimately shows the fractionation of the source rocks into a coarser fraction, transported along the channel bed and which, due to meager chemical weathering, is close to the dominant andesite. The finer size-fractions (i.e. TSS)

---

<sup>7</sup> The Los Altares gaging station is 230 km upstream from the city of Trelew and over 250 km from the estuary.

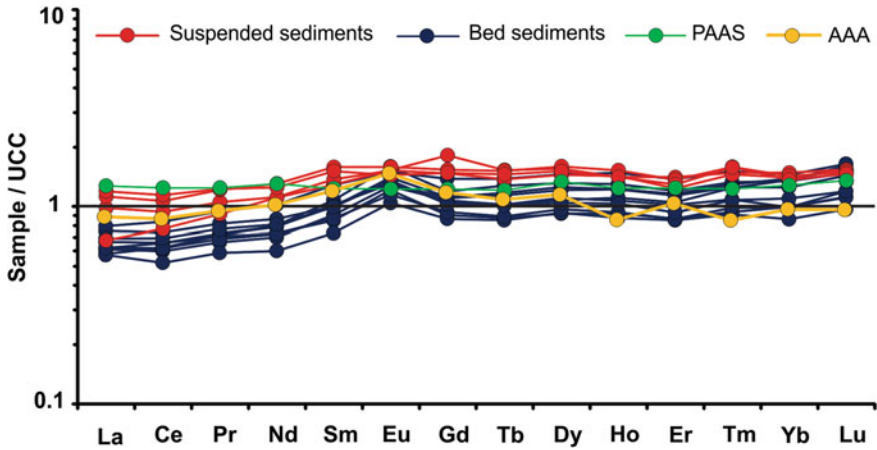


**Fig. 14** Rare earth element *spider diagrams* (i.e. or *spidergrams*) of Chubut River bed and suspended sediments, normalized to the upper continental crust (UCC). Bulk bed sediments are similar to a typical Andean andesite, whereas TSS resemble an average mudstone. Post-Archean Australian Shales (PAAS) from McLennan (1989), Average Andean Arc (AAA) from <http://www.geokem.com/>

represents the ultimate weathering product, which is enriched in REE in general (i.e. the higher specific surface area results in a higher adsorption), but in HREE in particular, and resembles typical mudstones (e.g. PAAS).

### 5 Summary and Final Comments

The Chubut is a medium size river, typical of Patagonia in several aspects: its active catchments are near the Andes, where it receives most of the atmospheric precipitations; it crosses eastbound the arid and wind-swept plateau, and annually delivers a rather limited freshwater volume (i.e.  $\sim 1.1 \text{ km}^3$ ) to the SW Atlantic. In operation since 1963, the Florentino Ameghino dam supplies hydroelectric power (46.9 MW) and irrigation, which mainly supports the intensive agricultural activities that take place in the lowermost valley. Human impact is, hence, mostly localized in the river's lower reach where two important cities—Trelew and Rawson—are located.

In the Chubut River upper catchments, atmospheric precipitations (i.e. rain- and snowfall) occur between May and August (austral fall and winter), when  $\sim 62\%$  of the total annual water volume is supplied to the drainage basin (Moyano and Moyano 2013). Accordingly, the discharge regime shows a mixed behavior in the upper gaging stations (i.e. Nacimiento, El Maitén, and Los Altares), accounted for by rainfall/snowfall in the (austral) winter months, and snow/ice melt, starting in September. The effect of the mountainous rain shadow—and the resulting aridity—is shown in the specific water yield, which varies from  $11.6 \text{ L s}^{-1} \text{ km}^{-2}$  (Nacimiento),

to  $13.5 \text{ L s}^{-1} \text{ km}^{-2}$  (El Maitén), down to  $2.2 \text{ L s}^{-1} \text{ km}^{-2}$  (Los Altares). The specific water yield becomes even lower at Valle Inferior ( $1.1 \text{ L s}^{-1} \text{ km}^{-2}$ ). The decrease in water yield is not only attributable to the increase of surface area, but also to the amplified consumptive use of water (i.e. water removed from the river that is evaporated, transpired by plants, incorporated into products or crops, consumed by humans or livestock, or otherwise removed from the Chubut River).

The Chubut's drainage basin is subjected to a *weathering-limited* denudation regime. Therefore, the mineral debris produced by erosion is scantily weathered and the mass of dissolved phases exported to the ocean is, hence, moderate.  $\text{TZ}^+$  fluctuates between *medium dilute* and *medium mineralized* water-type ( $1.5 < \text{TZ}^+ < 3.0 \text{ meq L}^{-1}$ ). *Dilute*-type waters ( $0.375 < \text{TZ}^+ < 0.75 \text{ meq L}^{-1}$ ) are common in mountainous tributary streams, as well as in the antecedent rivers crossing the Andes and flowing towards the Pacific coast. Glacial oligotrophic lakes, also pertaining in such drainage, display *very dilute* concentrations ( $0.185 < \text{TZ}^+ < 0.375 \text{ meq L}^{-1}$ ). *Dilute* and *very dilute* waters are of the  $\text{HCO}_3^- - \text{Ca}^{2+}$ -type, often with  $\text{SO}_4^{2-}$  as a subsidiary chemical species (i.e. possibly the result of subglacial pyrite oxidation). Downstream, in *medium dilute* or *medium mineralized* water-types,  $\text{Na}^+$ ,  $\text{SO}_4^{2-}$ , and  $\text{Cl}^-$  become more important components. The analysis of different water-mixing scenarios shows that: (a) the products of silicate weathering are ubiquitous; (b) given the abundance of glaciers in the headwaters, sulfide oxidation in subglacial conditions is likely to occur, generating  $\text{H}_2\text{SO}_4$  that attacks limestone and other rocks; (c) the information supplied by strontium isotopes indicates that it is linked with  $\text{Ca}^{2+}$  concentrations and it is mainly supplied by limestone dissolution; (d) a comparison with the analysis performed in the Sierra Nevada (USA) (Garrels and Mackenzie 1967) suggests variable time of contact between water and rock.

The REE geochemical signature of bed and suspended sediments shows the fractionation between coarse rock debris, sparsely attacked by chemical weathering processes, and the fine size-fraction (i.e. TSS), which is the final product of weathering processes, and bears a geochemical resemblance to typical mudstones.

## References

- Bouza PJ, Saín C, Videla L, Dell' Archiprete P, Cortés E, Rúa J (2017) Soil-geomorphology relationships in the Pichiñán uranium district, central region of Chubut Province, Argentina. In: Rabassa J (ed), *Advances in geomorphology and quaternary studies in Argentina*. Springer Earth System Sciences, Switzerland, pp 77–99
- Calmels D, Gaillardet J, Brenot A, France-Lanord C (2007) Sustained sulfide oxidation by physical erosion processes in the Mackenzie River basin: climatic perspectives. *Geology* 35(11):1003–1006
- Carson MA, Kirkby NJ (1972) *Hillslope form and processes*. Cambridge University Press
- Chillrud SN, Pedrozo FL, Temporetti PF, Planas HF, Froelich PN (1994) Chemical weathering of phosphate and germanium in glacial meltwater streams: Effects of subglacial pyrite oxidation. *Limnol Oceanogr* 39(5):1130–1140
- Davis JC (1986) *Statistics and data analysis in geology*. J Wiley & Sons, New York



- Depetris PJ, Gaiero DM, Probst J-L, Hartmann J, Kempe S (2005) Biogeochemical output and typology of rivers draining Patagonia's Atlantic seaboard. *J Coast Res* 21:835–844
- Depetris PJ, Pasquini AI (2008) Riverine flow and lake level variability in southern South America. *Eos* 89(28):254–255
- Depetris PJ, Pasquini AI, Lecomte KL (2014) *Weathering and the riverine denudation of continents*. Springer, Dordrecht
- Drever JI (1997) *The geochemistry of natural waters*. Prentice-Hall, Upper Saddle River
- Gaiero DM, Depetris PJ, Probst J-L, Bidart SM, Leleyter L (2004) The signature of river- and wind-borne materials exported from Patagonia to the southern latitudes: a view from REEs and implications for paleoclimatic interpretations. *Earth Planet Sci Lett* 219:357–376
- Gaiero DM, Probst J-L, Depetris PJ, Bidart SM, Leleyter L (2003) Iron and other transition metals in Patagonia river borne and windborne materials: geochemical control and transport to the southern South Atlantic Ocean. *Geochim Cosmochim Acta* 67:3606–3623
- Gaiero DM, Probst J-L, Depetris PJ, Leleyter L, Kempe S (2002) Riverine transfer of heavy metals from Patagonia to the southwestern Atlantic Ocean. *Reg Environ Chang* 3(1–3):51–64
- Gaillardet J, Dupré B, Louvat P, Allègre CJ (1999) Global silicate weathering and CO<sub>2</sub> consumption rates deduced from the chemistry of large rivers. *Chem Geol* 159:3–30
- Garrels RM, Mackenzie FT (1967) Origin of the chemical compositions of some springs and lakes. In: Gould RF (ed) *Equilibrium concepts in natural water systems*. American Chemical Society, Washington DC, pp 222–242
- Hernández MA, Ruiz de Galarreta VA, Fidalgo F (1983) Geohydrological diagnosis applied to the lower valley of Chubut River. *Ciencia Del Suelo* 1(2):83–91 (in Spanish)
- Hirsch RM, Slack JR (1984) A nonparametric trend test for seasonal data with serial dependence. *Water Resour Res* 20:727–732
- Kendall MG (1975) *Rank correlation methods*. Griffin, London
- Killops S, Killops V (2005) *Introduction to organic geochemistry*. Blackwell, Malden
- Langmuir D (1997) *Aqueous environmental geochemistry*. Prentice Hall, Upper Saddle River
- Ludwig W, Probst J-L (1998) River sediments discharge to the ocean: present-day controls and global budgets. *Am J Sci* 298:265–295
- Marsal D, Merriam DF (2014) *Statistics for geoscientists*. Elsevier, Amsterdam
- McLennan SN (1989) Rare earth elements in sedimentary rocks; influence of provenance and sedimentary processes. *Rev Mineral Geochem* 21:169–200
- McLennan SN (1993) Weathering and global denudation. *J Geol* 101:295–303
- Meybeck M (2005) Global occurrence of major elements in rivers. In: Drever JI (ed), *Surface and groundwater, weathering and soils*. Elsevier, Amsterdam
- Milliman JD, Farnsworth KL (2011) *River discharge to the coastal ocean. A global synthesis*, Cambridge
- Milliman JD, Meade RH (1983) World-wide delivery of river sediment to the ocean. *J Geol* 91:1–21
- Moyano CH, Moyano MC (2013) Hydrological study of the Chubut River. Upper and middle basin. *Contrib Cient Gæa* 251:149–164 (in Spanish)
- Pasquini AI (2000) *Geoquímica de sedimentos fluviales en una cuenca árida de alta latitud: el río Chubut, Patagonia, Argentina*. Doctoral dissertation. Universidad Nacional de Córdoba, Argentina (in Spanish)
- Pasquini AI, Depetris PJ (2007) Discharge trends and flow dynamics of South American rivers draining the southern Atlantic seaboard: An overview. *J Hydrol* 333:385–399
- Pasquini AI, Depetris PJ, Gaiero DM, Probst J-L (2005) Material sources, chemical weathering and physical denudation in the Chubut River basin (Patagonia, Argentina): implications for Andean rivers. *J Geol* 113:451–469
- Perdue EM, Ritchie JD (2005) Dissolved organic matter in freshwaters. In: Drever JI (ed) *Surface and groundwater, weathering and soils*. Elsevier, Amsterdam, pp 273–318
- Piper A (1944) A graphic procedure in the geochemical interpretation of water analyses. *Am Geophys Union Trans* 25:914–923

- Potter PE (1994) Modern sands of South America: composition, provenance and global significance. *Geol Rundsch* 83:212–232
- Rapela CW, Pankhurst RJ (2020) The continental crust of Northeastern Patagonia. *Ameghiniana* 57(5):480–498
- Sastre AV, Santinelli NH, Otaño SH, Ivanissevich ME (1998) Water quality in the lower section of the Chubut river, Patagonia, Argentina. *Verh Internat Verein Limnol* 26:951–955
- Scapini M del C, Orfila JD (2001). Características químicas de las aguas superficiales del Chubut. <http://www2.medioambiente.gov.ar/sian/chubut/trabajos/super.htm>. Accessed on 29 Apr 2020 (in Spanish)
- Subsecretaría de Recursos Hídricos (2002) Atlas Digital de los Recursos Hídricos Superficiales de la República Argentina, CD-Rom, Buenos Aires (in Spanish)
- Torres AI, Andrade CF, Moore WS, Faleschini M, Esteves JL, Niencheski LFH, Depetris PJ (2018) Ra and Rn isotopes as natural tracers of submarine groundwater discharge in the Patagonian coastal zone (Argentina): an initial assessment. *Environ Earth Sci* 77(4):145–154
- Tranter M (2005) Geochemical weathering in glacial and proglacial environments. In: Drever JI (ed) *Surface and groundwater, weathering and soils*. Elsevier, Amsterdam, pp 189–205